Unsplit Implementation of Higher Order PMLs

An unsplit implementation of Higher-Order PMLs for the seismic wave equation

David Connolly[1], Antonis Giannopoulos[1] and Mike Forde[1]

ABSTRACT

An unsplit recursive integration implementation of higher order PMLs for FDTD seismic modelling is presented. Firstly a new correction method PML implementation is outlined which allows the PML condition to be added directly to existing codes in a straightforward manner. Higher order PML equations are subsequently developed and implemented through a logical extension of the correction method. The resulting compact formula is capable of generating a PML condition of arbitrary order. The performance of a second order PML is tested against a similar first order implementation. It is found to have increased absorption performance for evanescent waves and waves at imaginary angles.

INTRODUCTION

Finite difference time domain (FDTD) modelling techniques are commonly used to simulate seismic wave propagation for the purposes of seismic exploration. Absorbing boundary conditions (ABC's) are typically used to prevent reflections from truncated domain edges contaminating results. The ABC performance dictates how far it should be placed from the modelling areas of concern. Therefore a highly effective ABC can significantly reduce the size of the computational domain and thus computational effort.

One wave equations [Higdon], optimal boundary conditions [Peng and Toksoz] and damping zone [cerjan] approaches have been attempted. Although these techniques generally perform well for waves arriving perpendicular to the boundary, their performance is reduced for waves impinging at low angles of incidence. This is undesirable for seismic wave modelling because the complex wave patterns are composed of large variations in incident angle.

Berenger introduced a 'Perfectly matched layer' (PML) technique to absorb electromagnetic waves based upon a series of finite layers, each with identical material properties, that gradually damp outgoing waves. This gradual damping is implemented through a stretching of the spatial coordinates inside the PML region. It offers high performance and is capable of absorbing waves independent of arrival angle. [chew and weedon] quickly extended the PML to include a stretching of both real and imaginary spatial co-ordinates thus offering the potential for additional absorption.

Using a similar implementation to electromagnetics, [chew and lui] adapted the PML condition to offer absorption for seismic waves. Despite this, spurious reflections were encountered for evanescent and low frequency waves. These shortcomings were addressed through the implementation of frequency dependant damping applied using the complex frequency shifted PML (C-PML) (x). C-PML techniques have since been developed for elastic(Komatitsch 2007), poroelastic(Martin 2008) and anisotropic media(becache 2003).

Early PML conditions (x) were implemented using an artificial splitting of velocity and stress fields. This splitting procedure made PML implementation in traditional FDTD codes challenging because two different sets of equations are required for each PML and non-PML region. In addition, such implementations are not well-posed (abarbanel).

To avoid field splitting, convolution terms (Komatitsch 2007), auxillary differential equations (Gedney 1998) and integral terms (Drossaert) have been proposed. As convolution is generally regarded as computationally inefficient, recent focus has shifted to auxillary differential equation (ADE) and integral term implementations.

(Martin 2010) outlines a non-convolutional ADE PML approach where a fourth-order Runge-Kutta scheme is used in conjunction with eighth order Holberg space discretization. This formulation is shown to have increased

[01]School of Engineering, University of Edinburgh, Kings buildings, AGB building, Edinburgh, EH9 3JF Scotland

accuracy over the traditional ADE-PML implementation and to be stable for up to 100,000 timesteps. Additionally [Martin] investigates the potential to extend this ADE-PML condition to higher order PML's but concludes that no significant performance benefit is capable.

(Zhang 2011) builds on the work of [martin 2010] and outlines a similar ADE-PML fourth-order Runge-Kutta scheme that results in a complete set of first order differential equations. This means that the same FDTD implementation can be used to solve both the ADE C-PML equations and the interior domain equations.

An alternative approach is outlined by [Drossaert] through the use of recursive integration (RIPML). This technique uses an extended trapezoidal rule to integrate the time derivates thus negating the requirement to split the fields or use an ADE formulation. RIPML requires an equal amount of memory in comparison to split formulations and slightly less memory than an ADE implementation.

Meanwhile, [correia, antonis] proposed a higher order PML implementation for Maxwell's equations. The additional degrees of freedom proved to offer superior absorption in comparison to traditional first order PML methods.

This paper extends the PML implementation described by [antonis] to the seismic wave equation using a RIPML approach. It has the potential to utilise a greater number of degrees of freedom in comparison to the traditional first order PML condition, thus offering greater absorption. It's increased performance is highlighted through several comparisons with an alternative first order PML condition.

IMPLEMENTING PML THROUGH A CORRECTION TECHNIQUE

Using a stretched coordinate system, the two-dimensional frequency domain elastodynamic velocity-stress equations take the form:

$$i\omega\tilde{v}_x = b\left(\frac{1}{s_x}\frac{\partial\tilde{\sigma}_{xx}}{\partial x} + \frac{1}{s_z}\frac{\partial\tilde{\sigma}_{xz}}{\partial z}\right) \quad (1)$$

$$i\omega\tilde{v}_z = b\left(\frac{1}{s_x}\frac{\partial\tilde{\sigma}_{xz}}{\partial x} + \frac{1}{s_z}\frac{\partial\tilde{\sigma}_{zz}}{\partial z}\right) \quad (2)$$

$$i\omega\tilde{\sigma}_{xx} = (\lambda+2\mu)\frac{1}{s_x}\frac{\partial\tilde{v}_x}{\partial x} + \lambda\frac{1}{s_z}\frac{\partial\tilde{v}_z}{\partial z} \quad (3)$$

$$i\omega\tilde{\sigma}_{zz} = (\lambda+2\mu)\frac{1}{s_z}\frac{\partial\tilde{v}_z}{\partial z} + \lambda\frac{1}{s_x}\frac{\partial\tilde{v}_x}{\partial x} \quad (4)$$

$$i\omega\tilde{\sigma}_{xz} = \mu\left(\frac{1}{s_x}\frac{\partial\tilde{v}_z}{\partial x} + \frac{1}{s_z}\frac{\partial\tilde{v}_x}{\partial z}\right) \quad (5)$$

Where velocity components are denoted by v and stress components by σ. λ and μ are the lames coefficients and b is buoyancy. Co-ordinate axis are defined by x and z.

s_x and s_z are the PML stretching functions, where

$$s_{u_i} = \kappa_{u_i} + \frac{d_{u_i}}{\alpha_{u_i} + i\omega} \quad (6)$$

and

$$\psi_u = \frac{1 - s_u}{s_u} \quad (7)$$

Rearranging equations 1-5 in terms of ψ_u gives

$$i\omega\tilde{v}_x = b\left((1+\psi_x)\frac{\partial\tilde{\sigma}_{xx}}{\partial x} - (1+\psi_z)\frac{\partial\tilde{\sigma}_{xz}}{\partial z}\right) \quad (8)$$

$$i\omega\tilde{v}_z = b\left((1+\psi_x)\frac{\partial\tilde{\sigma}_{xz}}{\partial x} - (1+\psi_z)\frac{\partial\tilde{\sigma}_{zz}}{\partial z}\right) \quad (9)$$

$$i\omega\tilde{\sigma}_{xx} = (\lambda+2\mu)(1+\psi_x)\frac{\partial\tilde{v}_x}{\partial x} - \lambda(1+\psi_z)\frac{\partial\tilde{v}_z}{\partial z} \quad (10)$$

$$i\omega\tilde{\sigma}_{zz} = (\lambda+2\mu)(1+\psi_z)\frac{\partial\tilde{v}_z}{\partial z} - \lambda(1+\psi_x)\frac{\partial\tilde{v}_x}{\partial x} \quad (11)$$

$$i\omega\tilde{\sigma}_{xz} = \mu\left((1+\psi_x)\frac{\partial\tilde{v}_z}{\partial x} - (1+\psi_z)\frac{\partial\tilde{v}_x}{\partial z}\right) \quad (12)$$

Examination reveals that the stretched velocity/stress equations are analogous to an addition of field dependant variables $\tilde{J}$ and $\tilde{M}$ to the original unstretched component.

$$i\omega\tilde{v}_x = b\left(\frac{\partial\tilde{\sigma}_{xx}}{\partial x} + \frac{\partial\tilde{\sigma}_{xz}}{\partial z}\right) + b\left(\tilde{J_{xx}} + \tilde{J_{xz}}\right) \quad (13)$$

$$i\omega\tilde{v}_z = \tilde{b}\left(\frac{\partial\tilde{\sigma}_{xz}}{\partial x} + \frac{\partial\tilde{\sigma}_{zz}}{\partial z}\right) + b\left(\tilde{J_{xz}} + \tilde{J_{zz}}\right) \quad (14)$$

$$i\omega\tilde{\sigma}_{xx} = (\lambda+2\mu)\frac{\partial\tilde{v}_x}{\partial x} + \lambda\frac{\partial\tilde{v}_z}{\partial z} + \left((\lambda+2\mu)\tilde{M_{xx}} + \lambda\tilde{M_{xz}}\right) \quad (15)$$

$$i\omega\tilde{\sigma}_{zz} = (\lambda+2\mu)\frac{\partial\tilde{v}_z}{\partial z} + \lambda\frac{\partial\tilde{v}_x}{\partial x} + \left((\lambda+2\mu)\tilde{M_{zz}} + \lambda\tilde{M_{zx}}\right) \quad (16)$$

$$i\omega\tilde{\sigma}_{xz} = \mu\left(\frac{\partial\tilde{v}_z}{\partial x} + \frac{\partial\tilde{v}_x}{\partial z}\right) + \mu\left(\tilde{M_{zx}} + \tilde{M_{xz}}\right) \quad (17)$$

Where $\tilde{J}$ and $\tilde{M}$ are given by

$$\tilde{J}_{xu} = \psi_u\frac{\partial\tilde{\sigma}_{xu}}{\partial u} \quad (18)$$

$$\tilde{M}_{xu} = \psi_u\frac{\partial\tilde{v}_v}{\partial u} \quad (19)$$

with $u,\ v \in \{x, z\}$ and $u \neq v$.

Velocity and stress values of the stretched coordinates in the PML region (i.e. where $\psi_u \neq 0$) can therefore be calculated through an addition of $\tilde{J}$ and $\tilde{M}$ to previously calculated values. This means that the PML can be implemented in existing scripts without revision of the original code.

DEVELOPMENT OF A HIGHER ORDER PML

In what follows, a PML formulation is derived for Nth order stretching. The approach avails of the previously defined correction PML implementation to allow for an efficient and straightforward implementation.

For brevity, only the derivation of J_{xz} is outlined. All other J_{uu} and M_{uu} can be found analogously.

Firstly,

$$s_u = \prod_{i=1}^{N} s_{u_i} \tag{20}$$

Assuming $u = z$ and $(1 - s_z)/s_z = \psi_z$ leads to

$$s_z \left(\tilde{J}_{xz} + \frac{\partial \tilde{\sigma}_{xz}}{\partial z} \right) = \frac{\partial \tilde{\sigma}_{xz}}{\partial z} \tag{21}$$

$$\left(\prod_{i=1}^{N} s_{z_i} \right) \left(\tilde{J}_{xz} + \frac{\partial \tilde{\sigma}_{xz}}{\partial z} \right) = \frac{\partial \tilde{\sigma}_{xz}}{\partial z} \tag{22}$$

To proceed with the derivation, a set of functions Ψ_{xz_i} are defined for $i \in [1, N-1]$

$$\Psi_{xz_i} = \left(\prod_{m=i+1}^{N} s_{z_m} \right) \left(\tilde{J}_{xz} + \frac{\partial \tilde{\sigma}_{xz}}{\partial z} \right) \tag{23}$$

Using equations x and y to eliminate $\tilde{J}_{xz}$, the following relationships are established:

$$\Psi_{xz_1} = \frac{1}{s_{z_1}} \frac{\partial \tilde{\sigma}_{xz}}{\partial z} \tag{24}$$

and

$$\Psi_{xz_i} = \frac{1}{s_{z_i}} \Psi_{i-1} \tag{25}$$

and finally,

$$\left(\tilde{J}_{xz} + \frac{\partial \tilde{\sigma}_{xz}}{\partial z} \right) = \frac{1}{s_{z_N}} \Psi_{xz_{N-1}} \tag{26}$$

for $i \in [2, N-1]$.

A substitution of s_{y_1} from X into Y gives

$$\kappa_{z_1} \Psi_{xz_1} + \frac{d_{z_1}}{\alpha_{z_1} + i\omega} \Psi_{xz_1} = \frac{\partial \tilde{\sigma}_{xz}}{\partial z} \tag{27}$$

With the intention of solving for Ψ_1, both sides are multiplied by $(\alpha_{z_1} + i\omega)$

$$(\alpha_{z_1}\kappa_{z_1} + d_{z_1})\Psi_{xz_1} + i\omega\kappa_{z_1}\Psi_{xz_1} = \alpha_{z_1} \frac{\partial \tilde{\sigma}_{xz}}{\partial z} + i\omega \frac{\partial \tilde{\sigma}_{xz}}{\partial z} \tag{28}$$

Before recursive integration takes place, X must be mapped from the frequency domain into the time domain. To prime X for transformation it is rearranged and similar terms are grouped together,

$$\Psi_{xz_1} = \frac{1}{\kappa_{z_1}} \frac{\partial \tilde{\sigma}_{xz}}{\partial z} + \frac{1}{i\omega} \Big[\frac{\alpha_{z_1}}{\kappa_{z_1}} \frac{\partial \tilde{\sigma}_{xz}}{\partial z} - \frac{(\alpha_{z_1}\kappa_{z_1} + d_{z_1})}{\kappa_{z_1}} \Psi_{xz_1} \Big] \tag{29}$$

The relationship $\frac{1}{i\omega}\tilde{A}(w) = \int_0^t A(t)\delta t$ can then be used to make the transform trivial

$$\Psi_{xz_1} = \frac{1}{\kappa_{z_1}} \frac{\partial \sigma_{xz}}{\partial z} + \int_0^t \frac{\alpha_{z_1}}{\kappa_{z_1}} \frac{\partial \sigma_{xz}}{\partial z} - \frac{(\alpha_{z_1}\kappa_{z_1} + d_{z_1})}{\kappa_{z_1}} \Psi_{xz_1}\, \delta t \tag{30}$$

It is assumed that the higher order PML will be implemented using a traditional velocity-stress FDTD grid that is staggered in both space and time. J_{uu} components are therefore evaluated at the same time instance as velocities (i.e. t = n) and M_{uu} components are evaluated at the same time instance as stresses (i.e. t = $n + 1/2$). It is also assumed that all field quantities are zero for $t \leq 0$. The index notation J_a^b, is utilised, where a defines the index for spatial discretization and b denoted the index for time discretization. Consequently the application of the extended trapezoidal rule results in:

$$\begin{aligned} \Psi_{xz_1}^{n+1/2} &= \frac{1}{\kappa_{z_1}} \frac{\partial \sigma_{xz}^{n+1/2}}{\partial z} + \\ &\sum_{p=0}^{n-1} \Big[\frac{\alpha_{z_1}\Delta t}{\kappa_{z_1}} \frac{\partial \sigma_{xz}^{p+1/2}}{\partial z} - \frac{(\alpha_{z_1}\kappa_{z_1} + d_{z_1})\Delta t}{\kappa_{z_1}} \Psi_{xz_1}^{p+1/2} \Big] \\ &+ \frac{\Delta t}{2} \frac{\alpha_{z_1}}{\kappa_{z_1}} \frac{\partial \sigma_{xz}^{n+1/2}}{\partial z} - \frac{\Delta t}{2} \frac{(\alpha_{z_1}\kappa_{z_1} + d_{z_1})}{\kappa_{z_1}} \Psi_{xz_1}^{n+1/2} \end{aligned} \tag{31}$$

rearranging yields

$$\begin{aligned} &\left(1 + \frac{\Delta t}{2} \frac{(\alpha_{z_1}\kappa_{z_1} + d_{z_1})}{\kappa_{z_1}} \right) \Psi_{xz_1}^{n+1/2} = \\ &\left(\frac{1}{\kappa_{z_1}} + \frac{\Delta t}{2} \frac{\alpha_{z_1}}{\kappa_{z_1}} \right) \frac{\partial \sigma_{xz}^{n+1/2}}{\partial z} + \\ &\sum_{p=0}^{n-1} \Big[\frac{\alpha_{u_1}\Delta t}{\kappa_{u_1}} \frac{\partial \sigma_{xz}^{p+1/2}}{\partial z} - \frac{(\alpha_{z_1}\kappa_{z_1} + d_{z_1})\Delta t}{\kappa_{z_1}} \Psi_{xz_1}^{p+1/2} \Big] \end{aligned} \tag{32}$$

Which is then solved for $\Psi_{xz_1}^{n+1/2}$

$$\begin{aligned} \Psi_{xz_1}^{n+1/2} &= \frac{2 + \Delta t\alpha_{z_1}}{2\kappa_{z_1} + \Delta t(\alpha_{z_1}\kappa_{z_1} + d_{z_1})} \frac{\partial \sigma_{xz}^{n+1/2}}{\partial z} + \\ &\frac{2\kappa_{z_1}}{2\kappa_{z_1} + \Delta t(\alpha_{z_1}\kappa_{z_1} + d_{z_1})} \sum_{p=0}^{n-1} \Big[\frac{\alpha_{z_1}\Delta t}{\kappa_{z_1}} \frac{\partial \sigma_{xz}^{p+1/2}}{\partial z} - \\ &\frac{(\alpha_{z_1}\kappa_{z_1} + d_{z_1})\Delta t}{\kappa_{z_1}} \Psi_{xz_1}^{p+1/2} \Big] \end{aligned} \tag{33}$$

Thus allowing $\Psi_{xz_1}^{n+1/2}$ to be obtained

$$\begin{aligned} \Psi_{xz_1}^{n+1/2} &= \frac{2 + \Delta t\alpha_{z_1}}{2\kappa_{z_1} + \Delta t(\alpha_{z_1}\kappa_{z_1} + d_{z_1})} \frac{\partial \sigma_{xz}^{n+1/2}}{\partial z} + \\ &\frac{2\kappa_{z_1}}{2\kappa_{z_1} + \Delta t(\alpha_{z_1}\kappa_{z_1} + d_{z_1})} \Phi_{xz_1}^{n-1/2} \end{aligned} \tag{34}$$

The value of the previous time integral is held by the summation memory variable Φ_{xz_1}. This variable is updated after the correction procedure of the FDTD field variables, but at the same time instance and thus within the same computational loop. It is defined by:

$$\Phi_{xz_1}^{n+1/2} = \Phi_{xz_1}^{n-1/2} + \frac{\alpha_{z_1}\Delta t}{\kappa_{z_1}}\frac{\partial \sigma_{xz}^{n+1/2}}{\partial z} - \frac{\Delta t(\alpha_{z_1}\kappa_{z_1} + d_{z_1})}{\kappa_{z_1}}\Psi_{xz_1}^{n+1/2} \tag{35}$$

The undesirable $\Phi_{xz_1}^{n+1/2}$ term can be eliminated from the update of $\Phi_{xz_1}^{n+1/2}$ via x and y, resulting in:

$$\Phi_{xz_1}^{n+1/2} = \frac{2\kappa_{z_1} - \Delta t(\alpha_{z_1}\kappa_{z_1} + d_{z_1})}{2\kappa_{z_1} + \Delta t(\alpha_{z_1}\kappa_{z_1} + d_{z_1})}\Phi_{xz_1}^{n-1/2} - \frac{2d_{z_1}\Delta t}{(2\kappa_{z_1} + \Delta t(\alpha_{z_1}\kappa_{z_1} + d_{z_1}))\kappa_{z_1}}\frac{\partial \sigma_{xz}^{n+1/2}}{\partial z} \tag{36}$$

Upon inspection of X, it is seen than for $i \in [2, N-1]$, all Ψ_{xz_i} can be calculate in an analogous manner to Ψ_{xz_1} resulting in

$$\Psi_{xz_i}^{n+1/2} = \frac{2 + \Delta t\alpha_{z_i}}{2\kappa_{z_i} + \Delta t(\alpha_{z_i}\kappa_{z_i} + d_{z_i})}\Psi_{xz_{i-1}}^{n+1/2} + \frac{2\kappa_{z_i}}{2\kappa_{z_i} + \Delta t(\alpha_{z_i}\kappa_{z_i} + d_{z_i})}\Phi_{xz_i}^{n-1/2} \tag{37}$$

correspondingly, the previous time integrals, Φ_{xz_i} for $i \in [2, N]$ can be updated:

$$\Phi_{xz_i}^{n+1/2} = \frac{2\kappa_{z_i} - \Delta t(\alpha_{z_i}\kappa_{z_i} + d_{z_i})}{2\kappa_{u_i} + \Delta t(\alpha_{z_i}\kappa_{z_i} + d_{z_i})}\Phi_{xz_i}^{n-1/2} - \frac{2\sigma_{z_i}\Delta t}{(2\kappa_{z_i} + \Delta t(\alpha_{z_i}\kappa_{z_i} + d_{z_i}))\kappa_{z_i}}\Psi_{xz_{i-1}}^{n+1/2} \tag{38}$$

Furthermore, through an application of the same principles as used to develop eqs x and y, x and y themselves can be compared to Z thus providing an overall formulation for J_{xz}

$$J_{xz}^{n+1/2} = \frac{2 + \Delta t\alpha_{z_N}}{2\kappa_{z_N} + \Delta t(\alpha_{z_N}\kappa_{z_N} + d_{z_N})}\Psi_{xz_{N-1}}^{n+1/2} + \frac{2\kappa_{z_N}}{2\kappa_{z_N} + \Delta t(\alpha_{z_N}\kappa_{z_N} + d_{z_N})}\Phi_{xz_N}^{n-1/2} - \frac{\partial \sigma_{xz}^{n+1/2}}{\partial z} \tag{39}$$

Because Ψ_{xz_i} is merely a function of both $\partial\sigma_{xz_1}/\partial z$ and Φ_{xz_1}, Ψ_{xz_i} can be eliminated from x. Finally, the creation of four new variables, RA_{z_i}, RB_{z_i}, RC_{z_i} and RD_{z_i} results in the compact formula:

$$J_{xz}^{n+1/2} = \left\{\left(\prod_{q=1}^{N}\mathrm{RA}_{z_q}\right) - 1\right\}\frac{\partial \sigma_{xz}^{n+1/2}}{\partial z} + \sum_{i=1}^{N-1}\left\{\left(\prod_{q=i+1}^{N}\mathrm{RA}_{z_q}\right)\mathrm{RB}_{z_i}\Phi_{xz}^{n-1/2}\right\} + \mathrm{RB}_{z_N}\Phi_{xz_N}^{n-1/2} \tag{40}$$

where $i \in [2, N-1]$.

Similarly, due to the same relationship between Ψ_{xz_i}, $\partial\sigma_{xz_1}/\partial z$ and Φ_{xz_1}, Ψ_{xz_i} can be eliminated from the summation memory variable.

$$\Phi_{xz_i}^{n+1/2} = \mathrm{RE}_{z_i}\Phi_{xz_i}^{n-1/2} - \mathrm{RF}_{z_i}\left\{\left(\prod_{q=1}^{i-1}\mathrm{RA}_{z_q}\right)\frac{\partial \sigma_{xz}^{n+1/2}}{\partial z} + \sum_{m=1}^{i-1}\left(\prod_{q=m+1}^{i-1}\mathrm{RA}_{z_q}\right)\mathrm{RB}_{z_m}\Phi_{xz_m}^{n-1/2}\right\} \tag{41}$$

Also where $i \in [2, N-1]$. RA_{z_i}, RB_{z_i}, RC_{z_i} and RD_{z_i} are defined by:

$$\begin{aligned}
\mathrm{RA}_{z_i} &= \frac{2 + \Delta t\alpha_{z_i}}{2\kappa_{z_i} + \Delta t(\alpha_{z_i}\kappa_{z_i} + d_{z_i})} \\
\mathrm{RB}_{z_i} &= \frac{2\kappa_{z_i}}{2\kappa_{z_i} + \Delta t(\alpha_{z_i}\kappa_{z_i} + d_{z_i})} \\
\mathrm{RE}_{z_i} &= \frac{2\kappa_{z_i} - \Delta t(\alpha_{z_i}\kappa_{z_i} + d_{z_i})}{2\kappa_{z_i} + \Delta t(\alpha_{z_i}\kappa_{z_i} + d_{z_i})} \\
\mathrm{RF}_{z_i} &= \frac{2\sigma_{z_i}\Delta t}{(2\kappa_{z_i} + \Delta t(\alpha_{z_i}\kappa_{z_i} + d_{z_i}))\kappa_{z_i}}
\end{aligned}$$

First order implementation

$$J_{xz}^{n+1/2} = \left\{\mathrm{RA}_{z_1} - 1\right\}\frac{\partial \sigma_{xz}^{n+1/2}}{\partial z} + \mathrm{RB}_{z_1}\Phi_{xz_1}^{n-1/2} \tag{42}$$

followed by the update of Φ_1

$$\Phi_{xz_1}^{n+1/2} = \mathrm{RE}_{z_1}\Phi_{xz_1}^{n-1/2} - \mathrm{RF}_{z_1}\frac{\partial \sigma_{xz}^{n+1/2}}{\partial z} \tag{43}$$

Second order implementation

$$J_{xz}^{n+1/2} = \left\{\mathrm{RA}_{z_1}\mathrm{RA}_{z_2} - 1\right\}\frac{\partial \sigma_{xz}^{n+1/2}}{\partial z} + \mathrm{RA}_{z_2}\mathrm{RB}_{z_1}\Phi_{xz_1}^{n-1/2} + \mathrm{RB}_{z_2}\Phi_{xz_2}^{n-1/2} \tag{44}$$

followed by the updates for Φ_{xz_2} and Φ_{xz_1}

$$\Phi_{xz_2}^{n+1/2} = \mathrm{RE}_{z_2}\Phi_{xz_2}^{n-1/2} - \mathrm{RF}_{z2}\left\{\mathrm{RA}_{z_1}\frac{\partial \sigma_{xz}^{n+1/2}}{\partial z} + \mathrm{RB}_{z_1}\Phi_{xz_1}^{n-1/2}\right\}$$

$$\Phi_{xz_1}^{n+1/2} = \mathrm{RE}_{z_1}\Phi_{xz_1}^{n-1/2} - \mathrm{RF}_{z_1}\frac{\partial \sigma_{xz}^{n+1/2}}{\partial z}$$

PML STABILITY

Although it has been shown in X that second order PML's can provide enhanced performance over first order PML's for electromagnetic wave absorption, it is still unclear as to whether PML orders greater than second provide any significant benefit. Therefore this work will primarily focus upon second order implementation and testing. For this case, two approaches are utilised to maximise absoption, a combination of the classical and CFS PML stretching functions, and a combination of two CFS stretching

functions.

The stretching functions are defined as:

$$s_{classical} = \kappa + \frac{d}{i\omega} \tag{45}$$

$$s_{CFS} = \kappa + \frac{d}{\alpha + i\omega} \tag{46}$$

$$s_{classical-CFS} = \left(\kappa + \frac{d}{i\omega}\right)\left(\kappa + \frac{d}{\alpha + i\omega}\right) \tag{47}$$

$$s_{CFS-CFS} = \left(\kappa + \frac{d}{\alpha + i\omega}\right)\left(\kappa + \frac{d}{\alpha + i\omega}\right) \tag{48}$$

Stretching function parameters have a significant effect in a PML's ability attenuate wave energy. Careless parameter selection can also lead to instability, especially as PML order increases. To determine stability criterion the real part of the stretching function must be greater or equal to 1 or the PML will cause a physical contraction of space rather than a stretching of space. Similarly, the imaginary part must be greater than zero or the PML region will experience a magnification of amplitude rather than an attenuation. This can be expressed as:

$$r_{O2} \geq 1 \tag{49}$$

and

$$I_{O2} \geq 0 \tag{50}$$

CLASSICAL-CFS STABILITY CRITERION

X found that for the absoption of electromagnetic waves, optimum performance was achieved by combining classical and CFS stretching functions (equation x). It is postulated that for some domains, combining the standard PML's ability to absorb frequency independant waves with the CFS-PML's ability to absorb low frequency evanescent waves, greater performance is achievable.

The real and imaginary components for this case can be shown to be:

$$r_{O2} = \kappa_2 + \frac{d_2\alpha_2}{\alpha_2^2 + \omega^2} - \frac{d_1 d_2}{\alpha_2^2 + \omega^2} \tag{51}$$

$$I_{O2} = \frac{d_1\kappa_2}{\omega} + \frac{d_2\omega}{\alpha_2^2 + \omega^2} + \frac{d_1 d_2 \alpha_2}{\omega(\alpha_2^2 + \omega^2)} \tag{52}$$

To fulfill these criterea it can be observed that careful choices of α_2 and κ_2 must be made ($\alpha_2 > d_1$ and $\kappa_2 \geq 1$). These conditions must be fulfilled at every point within the PML domain meaning parameters must be graded carefully. A grading approach similar to that presented by Komatitsch was found to give high performance.

$$d_{j_N} = d_{0_N}(\frac{j}{L})^{a_N} \tag{53}$$

$$\kappa_{j_N} = 1 + (\kappa_{max_N} - 1)^{b_N} \tag{54}$$

$$\alpha_{j_N} = \alpha_{max_N}(1 - (\frac{j}{L})^{c_N}) \tag{55}$$

where $j \in [x, y, z]$, N is the PMl order and L is the thickness of the PML layer. Lastly, $d_0 = \frac{3v_p}{2L} log\frac{1}{R}$ where v_p is the maximum compressional wave speed and R is the theoretical reflection coefficient.

In contrast to Komatitsch, a non-reversed α_2 scaling has been used resulting in the minimum α_2 value being located at the intersection between PML and modelling space, and the maximum value being located on the outer extremity of the PML. Physically this means that α_2 is graded in the same direction to d_1, making it trivial to ensure $\alpha_2 > d_1$, thus fulfilling the stability criterion.

CFS-CFS STABILITY CRITERION

The CFS-CFS PML approach has a greater number of degrees of freedom in comparison to the RI-CFS-PML because the additional α_1 and κ_1 coefficients are utilised. Therefore for some domains the CFS-CFS PML may also provide enhanced abroption.

The real and imaginary parts of the stretching function:

$$r_{O2} = \kappa_1\kappa_2 + \frac{\alpha_2\kappa_1 d_2}{\alpha_2^2 + \omega^2} + \frac{\alpha_1\kappa_2 d_1}{\alpha_1^2 + \omega^2} + \left(\frac{\alpha_1\alpha_2}{(\alpha_1^2 + i\omega^2)(\alpha_2^2 + i\omega^2)} - \frac{\omega^2}{(\alpha_1^2 + I\omega^2)(\alpha_2^2 + i\omega^2)}\right) d_1 d_2 \tag{56}$$

$$I_{O2} = \frac{\kappa_1\omega d_2}{(\alpha_2^2 + i\omega^2)} + \frac{d_1\omega\kappa_2}{(\alpha_1^2 + i\omega^2)} - \left(\frac{\alpha_2\omega}{(\alpha_1^2 + \omega^2)(\alpha_2^2 + \omega^2)} + \frac{\alpha_1\omega}{(\alpha_1^2 + \omega^2)(\alpha_2^2 + \omega^2)}\right) d_1 d_2 \tag{57}$$

Assuming that all PML coefficient values are chosen to be positive the imaginary part of the stretching function will always be fulfilled. Despite this, unlike the classical-CFS case, the stability of the real part of the CFS-CFS stretching function is frequency dependant. Therefore to maintain stability, $\alpha_1 \cdot \alpha_2 > \omega^2$, and $\kappa_2 \geq 1$.

Unlike the Classical-CFS stretching function, α_2 scaling must be considered relative to α_1 scaling to ensure that the stability critereon is met at every grid point within the PML region. Once again, if both α_1 and α_2 are scaled from a minimum at the threshold between PML and modelling space, to a maximum at the PML extremity then it is straightforward to ensure the stability condition is met.

Although the CFS-CFS stability criterion is slightly more challenging to meet, the absoption performance benefits can be significant as will be shown.

NUMERICAL RESULTS

CORRECTION PML PERFORMANCE

CORRECTION PML VS ORIGINAL FORMULATION

The correction PML implementation was tested against the original recursive integration implementation as described in (Drossaert). Although both formulations are similar the correction version allows for a more straightforward implementation. Numerous numerical experiments were conducted including those outlined in (Drossaert). Both formulations were found to perform nearly identically and due to the high similarity the resulting traces are omitted. The only discrepancies were in the range of (1 x 10^{15}) generated due to numerical precision errors arrising from the different implementations.

CORRECTION PML VS CPML

The correction PML implementation was benchmarked against the CPML implementation as described in (Martin x 2). The new formulation was tested using a homogenous, two dimensional rectangular grid identical to that also outlined in (Martin). The domain comprised of 101 x 641 square cells, with 10m spacing between grid points in both directions. The homogenous material was characterised by pressure wave velocity $c_p = 3300\ ms^{-1}$, shear wave velocity $c_s = 1905\ ms^{-1}$ and density $\rho = 2800$ kgm^{-3}. The staggered computational scheme was second order accurate in both space and time with a constant time step of $\delta t = 0.001s$. The grid followed that outlined by Virieux and was bounded on all sides by a PML region 10 cells thick.

A 8Hz excitation with the form of a first derivative of a gaussian was used to excite the velocity components in both directions at coordinate (79, 427). Recievers one, two and three were placed at (20,413), (70,227) and (81,27) respectively. Physically receiver one was located closest to the source and receiver three located furthest away (Figure 1).

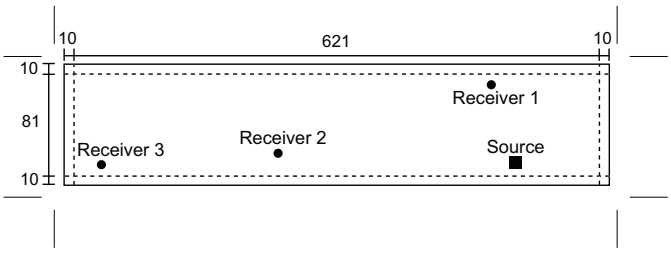

Figure 1: Model schematic (rotated 90^o)

For both implementations PML parameters were taken from Martin who showed that using $\kappa_{max} = 7$ and $\alpha_{max} = \omega\pi$ facilitated high CFS absorption performance for this particular domain. Additionally, $d_{max} = \frac{3v_p}{2L} log\frac{1}{R}$ where v_p = compressional wave speed, L = number of PML layers and R is the reflection coefficient (R = 1 x 10^{-5}).

Once again for this example the resulting traces were similar. Therefore to facilitate a more detailed comparison of performance a metric is introduced:

$$\text{Error}_{\text{db}}|^n_{i,j} = 20\log_{10}\frac{\|E|^n_{i,j} - E_{\text{ref}}|^n_{i,j}\|}{\|E_{\text{ref}_{\text{max}}}|_{i,j}\|} \tag{58}$$

Where $E^n_{i,j}$ represents the test trace at a point in time n and at spatial location i, j. E_{ref} represents the reference solution, and $E_{ref_{max}}$ is the maximum amplitude of the reference trace. When plotted this allows for a better visual interpretation of the errors at each point in time.

Although the error plots (Figure X) allow for easier comparison between traces, there are still large similarities between results. At some points the CPML can be seen to perform marginly better but at other points the correction PML exhibits slightly higher accuracy. This is clearly evident at receivers vx1 and vx2. Therefore it can be concluded that the CPML offers very similar performance to the CPML implementation.

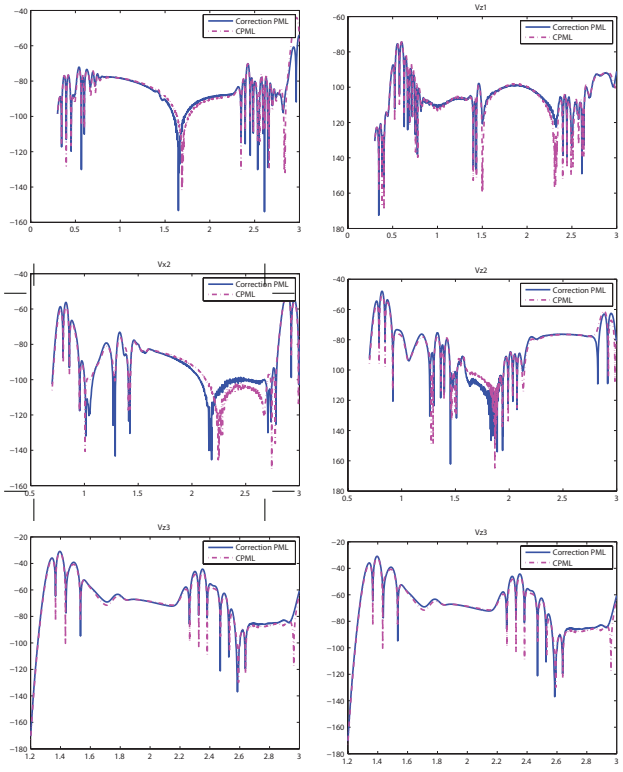

Figure 2: Error plots - CPML vs correction PML

SECOND ORDER PML PERFORMANCE

To illustrate the ability of a higher order PML scheme to outperform its first order counterpart, a CFS-CFS stretching function was tested to determine whether combining these optimised parameters with an additional CFS stretching function would offer increased performance. The second set of CFS parameters were as follows:

$$d_{max_2} = \frac{d_{max_1}}{30} \tag{59}$$

$$\kappa_{max_2} = 1.5 \tag{60}$$

$$\alpha_{max_2} = 2d_{max_1} \tag{61}$$

Figure 2 shows the velocity trace comparisons however due to the high performance of both schemes, performance is indistinguishable.

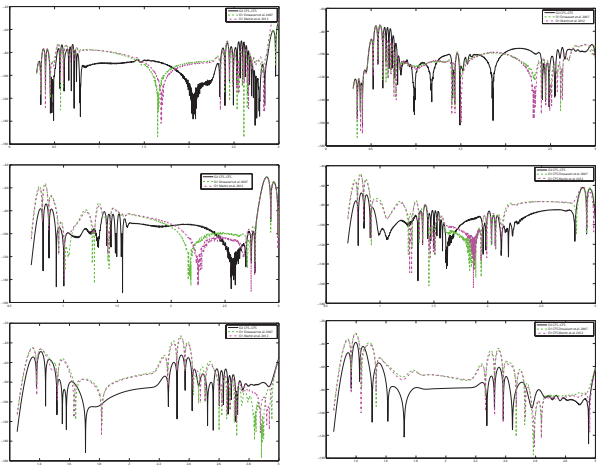

Figure 3: Experimental error plots

Figure X shows the resulting error plots. Both first order CFS formulations produce nearly identical results and it can be seen that the overall error increases as the receiver distance is increased. Concerning the O2 CFS-CFS implementation, performance at receivers vx_1 and vz_1 is improved slightly but for as distance increases, performance increases rapidly. Receivers vx_3 and vz_3 show a marked improvement with on average between 10dB and 20dB less error.

The furthest away receivers are subject to a greater number of evanescent waves and waves arriving at imaginary angles in comparison to the closest receivers. PML schemes typically have degraded performance under such conditions but the additional degrees of freedom associated with the O2 PML allow it to maintain higher levels of performance in comparison to both CFS stretching functions.

As the close receivers experience only a low percentage of these waves the first order CFS is capable of high performance absorption. Therefore there is not much scope for improvement by adding an additional stretching function.

It should be noted that attempts were also made to improve absorption performance using the classical-CFS stretching function. Despite this no significant performance benefits were found.

SECOND ORDER PML STABILITY

The importantance of fulfilling the stability critereon for both the Classical-CFS and CFS-CFS stretching functions were examined also using the example presented by (Martin).

CLASSICAL-CFS STABILITY

For this example the classcial parameters were, $d_{1_{max}} = 569.9$, $\kappa_{1_{max}} = 1$, $\alpha_{1_{max}} = 0$ and the second order CFS parameters were chosen as $d_{2_{max}} = d_{1_{max}}$, $\kappa_{2_{max}} = 20$, $\alpha_{2_{max}} = \gamma d_{1_{max}}$, where $\gamma \in \{0.02, 0.05, 0.1, 1, 2, 5\}$.

Figure X shows a trace comparison between several $\alpha_{2_{max}}$ values and the response calculated using the optimised CFS-CFS parameters from section X. Observation point vz3 has been chosen because it is located far from the source and instabilities are thus most evident. It is seen that as $\alpha_{2_{max}}$ deviates from the recommended value of $\sigma_{1_{max}}$, performance is radically reduced and stabilities occur. This is because as $\alpha_{2_{max}}$ decreases the corresponding real part of the stretching function becomes more negative (Figure X).

It should be noted that to maintain stability using (equation x), α_2 must be scaled from a minimum at the pml/domain interface to a maximum at the extremity of the computational grid. If not, the stability critereon will only be partially fulfilled, i.e. it will be fulfilled for locations close to the pml/domain interface but not for regions close to the grid edge.

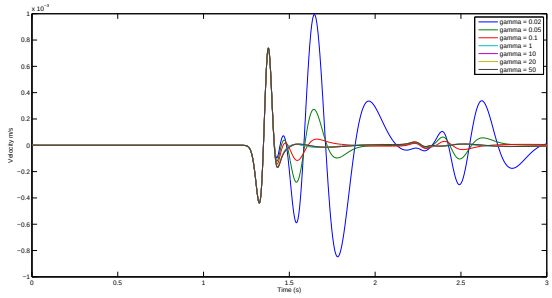

Figure 4: The effect of $\alpha_{2_{max}}$ on Classical-CFS PML

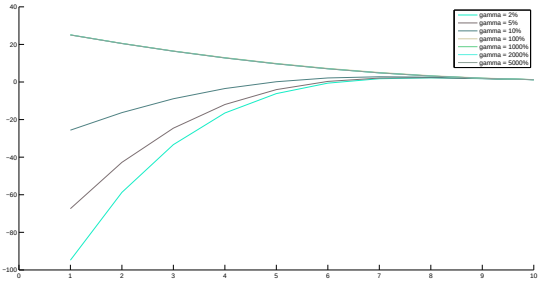

Figure 5: Real component of the Classical-CFS stretch

CFS-CFS STABILITY

To analyse stability the following parameters were chosen: $d_{1_{max}} = 569.9,\ \kappa_{1_{max}} = 7,\ \alpha_{1_{max}} = \zeta,\ d_{2_{max}} = \frac{d_{2_{max}}}{30},\ \kappa_{2_{max}} = 1.5,\ \alpha_{2_{max}} = \zeta.\ \zeta = \sqrt{(}\gamma 2\pi w)$.

APPENDIX A

HIGHER ORDER PML'S FOR A GENERAL 3D CASE

For a staggered scheme where velocity components are updated at $t = n$ and stress components are updated at $t = n + 1/2$, the calculation of velocity for the entire grid is as follows:

$$v_i^n = v_i^{n-1} + b\delta t(J_{ii}^n + J_{ij}^n + J_{ik}^n) \tag{A-1}$$

where δt is the timestep size and $i, j, k \in [x, y, z]$. The PML velocity correction terms J_{ii}, J_{ij}, J_{ik} are calculated using

$$J_{ij}^n = \left\{ \left(\prod_{q=1}^{N} \mathrm{RA}_{j_q} \right) - 1 \right\} \frac{\partial d_{ij}^n}{\partial j} + \sum_{p=1}^{N-1} \left\{ \left(\prod_{q=p+1}^{N} \mathrm{RA}_{j_q} \right) \mathrm{RB}_{j_p} \Phi_{ij}^{n-1} \right\} + \mathrm{RB}_{j_N} \Phi_{ij_N}^{n-1} \tag{A-2}$$

where N is the order of PML and $p \in [1, N]$. The previous time integral $\Phi_{ij_p}^n$ is obtained through

$$\Phi_{ij_p}^n = \mathrm{RE}_{j_p} \Phi_{ij_p}^{n-1} - \mathrm{RF}_{j_p} \left\{ \left(\prod_{q=1}^{p-1} \mathrm{RA}_{j_q} \right) \frac{\partial d_{ij}^n}{\partial j} + \sum_{m=1}^{p-1} \left(\prod_{q=m+1}^{p-1} \mathrm{RA}_{j_q} \right) \mathrm{RB}_{j_m} \Phi_{ij_m}^{n-1} \right\} \tag{A-3}$$

Similarly, stresses at $t = n+1/2$ can then be calculated using

$$d_{ij}^{n+1/2} = d_{ij}^{n+1/2} + \delta t C_{ijkl}(M_{ii}^{n+1/2} + M_{ij}^{n+1/2} + M_{ik}^{n+1/2}) \tag{A-4}$$

with the correction terms found using

$$M_{ij}^{n+1/2} = \left\{ \left(\prod_{q=1}^{N} \mathrm{RA}_{j_q} \right) - 1 \right\} \frac{\partial v_j^{n+1/2}}{\partial j} + \sum_{p=1}^{N-1} \left\{ \left(\prod_{q=p+1}^{N} \mathrm{RA}_{j_q} \right) \mathrm{RB}_{j_p} \Phi_{ij}^{n-1/2} \right\} + \mathrm{RB}_{j_N} \Phi_{ij_N}^{n-1/2} \tag{A-5}$$

and the previous time integral

$$\Phi_{ij_p}^{n+1/2} = \mathrm{RE}_{j_p} \Phi_{ij_p}^{n-1/2} - \mathrm{RF}_{j_p} \left\{ \left(\prod_{q=1}^{p-1} \mathrm{RA}_{j_q} \right) \frac{\partial v_j^{n+1/2}}{\partial j} + \sum_{m=1}^{p-1} \left(\prod_{q=m+1}^{p-1} \mathrm{RA}_{j_q} \right) \mathrm{RB}_{j_m} \Phi_{ij_m}^{n-1/2} \right\} \tag{A-6}$$

For all J_{ij}^n and $M_{ij}^{n+1/2}$,

$$\begin{aligned} \mathrm{RA}_{z_p} &= \frac{2 + \Delta t \alpha_{z_p}}{2\kappa_{z_p} + \Delta t(\alpha_{z_p}\kappa_{z_p} + d_{z_p})} \\ \mathrm{RB}_{z_p} &= \frac{2\kappa_{z_p}}{2\kappa_{z_p} + \Delta t(\alpha_{z_p}\kappa_{z_p} + d_{z_p})} \\ \mathrm{RE}_{z_p} &= \frac{2\kappa_{z_p} - \Delta t(\alpha_{z_p}\kappa_{z_p} + d_{z_p})}{2\kappa_{z_p} + \Delta t(\alpha_{z_p}\kappa_{z_p} + d_{z_p})} \\ \mathrm{RF}_{z_p} &= \frac{2 d_{z_p} \Delta t}{(2\kappa_{z_p} + \Delta t(\alpha_{z_p}\kappa_{z_p} + d_{z_p}))\kappa_{z_p}} \end{aligned}$$

Outwith the PML region $d = 0, \alpha = 0, \kappa = 1$, resulting in $RA = 1, RB = 1, RE = 1, RF = 0$. This causes J_{ii}, J_{ij}, J_{ik} to reduce to $\partial d_{ij}^n / \partial z$ and M_{ii}, M_{ij}, M_{ik} to reduce to $\partial v_j^{n+1/2} / \partial z$. Therefore both stress and velocity equations automatically revert to the original stress derivatives.